

Reducing uncertainty in the climatic interpretations of speleothem $\delta^{18}\text{O}$

C. N. Jex,^{1,2,3} S. J. Phipps,^{4,5} A. Baker,^{2,3} and C. Bradley⁶

Received 4 February 2013; revised 11 April 2013; accepted 11 April 2013; published 21 May 2013.

[1] We explore two principal areas of uncertainty associated with paleoclimate reconstructions from speleothem $\delta^{18}\text{O}$ ($\delta^{18}\text{O}_{\text{spel}}$): potential non-stationarity in relationships between local climate and larger-scale atmospheric circulation, and routing of water through the karst aquifer. Using a $\delta^{18}\text{O}_{\text{spel}}$ record from Turkey, the CSIRO Mk3L climate system model and the KarstFOR karst hydrology model, we confirm the stationarity of relationships between cool season precipitation and regional circulation dynamics associated with the North Sea-Caspian pattern since 1 ka. Stalagmite $\delta^{18}\text{O}$ is predicted for the last 500 years, using precipitation and temperature output from the CSIRO Mk3L model and synthetic $\delta^{18}\text{O}$ of precipitation as inputs for the KarstFOR model. Interannual variability in the $\delta^{18}\text{O}_{\text{spel}}$ record is captured by KarstFOR, but we cannot reproduce the isotopically lighter conditions of the sixteenth to seventeenth centuries. We argue that forward models of paleoclimate proxies (such as KarstFOR) embedded within isotope-enabled general circulation models are now required. **Citation:** Jex, C. N., S. J. Phipps, A. Baker, and C. Bradley (2013), Reducing uncertainty in the climatic interpretations of speleothem $\delta^{18}\text{O}$, *Geophys. Res. Lett.*, 40, 2259–2264, doi:10.1002/grl.50467.

1. Introduction

[2] Speleothem $\delta^{18}\text{O}$ ($\delta^{18}\text{O}_{\text{spel}}$) is an excellent proxy for terrestrial paleoclimate reconstruction. The $\delta^{18}\text{O}$ of cave drip water ($\delta^{18}\text{O}_{\text{dw}}$) from which a speleothem forms records the isotopic composition of the proportion of water that infiltrates into the deep soil layers and karst aquifer. Statistical relationships between $\delta^{18}\text{O}_{\text{spel}}$ and specifically the amount of observed precipitation have been used to generate quantitative hydroclimate reconstructions in regions where there is a reliable isotopically distinct seasonal recharge of ground water [Baker et al., 2007; Cai et al., 2010; Jex et al., 2010; Matthey et al., 2008; Yadava et al., 2004]. Such reconstructions depend upon two key assumptions. First, the application of

statistically derived relationships beyond calibration-validation time periods assumes their stationarity. Second, any climatic interpretations also assume that the dominant patterns of atmospheric circulation and the seasonal distribution of precipitation have remained stable in nature throughout the period of study [Sturm et al., 2010]. The first assumption may be addressed by forward modeling a $\delta^{18}\text{O}$ pseudoproxy time series [Sturm et al., 2010], whilst the second assumption can be tested by examining the relationships between local climate parameters and atmospheric circulations during and beyond the instrumental period using a climate system model.

[3] Published models to predict $\delta^{18}\text{O}_{\text{dw}}$ include the oxygen isotope drip water and stalagmite model (ODSM) [Wackerbarth et al., 2010] and the KarstFOR karst hydrology model [Baker et al., 2012]. Both have been used to predict $\delta^{18}\text{O}_{\text{dw}}$ and $\delta^{18}\text{O}_{\text{spel}}$ during the last century [Baker and Bradley, 2010; Baker et al., 2012; Lohmann et al., 2013], and beyond the instrumental period [Baker et al., 2012; Wackerbarth et al., 2012; Baker et al., manuscript in revision]. They consider infiltration of precipitation due to evapotranspiration and evaporative fractionation in soil water and predict $\delta^{18}\text{O}_{\text{dw}}$. KarstFOR is a lumped parameter karst hydrology model, which, unlike ODSM, allows for seepage and preferential routing of water through five water stores. Input series are temperature (T) and precipitation (P) and $\delta^{18}\text{O}$ of precipitation ($\delta^{18}\text{O}_{\text{pptn}}$). The model generates time series for $\delta^{18}\text{O}_{\text{dw}}$ and $\delta^{18}\text{O}$ of speleothem calcite ($\delta^{18}\text{O}_{\text{cmod}}$; following Kim and O'Neil [1997]) that may be attributed to changes in the seasonality of recharge arising from a modified potential evapotranspiration (PET) regime imposed by changing T and P. This avoids the assumption of stationarity inherent in statistically derived relationships. Similarly, storage times and evaporative fractionation of $\delta^{18}\text{O}_{\text{pptn}}$ predicted in the soil zone may be modeled, as well as varying residence times, storage capacity, and the subsequent routing and mixing of old and young groundwater in the karst aquifer. So far, studies using the KarstFOR model have confirmed the importance of considering water balance in PET sensitive regions and identified non-stationarity in $\delta^{18}\text{O}_{\text{spel}}$ due to changing water balance.

[4] Here we present the results of a multi-model proxy comparison using KarstFOR in conjunction with a climate system model, to demonstrate how interpretations based on $\delta^{18}\text{O}_{\text{spel}}$ records may be refined and key uncertainties addressed. We use a published speleothem record used to reconstruct the amount of cool season precipitation of the last 500 years using linear regression methods [Jex et al., 2011] and the CSIRO Mk3L climate system model, a reduced-resolution coupled general circulation model, designed primarily for millennial-scale climate simulation and paleoclimate research [Phipps et al., 2011, 2012]. The speleothem sample (2p) is from Akçakale cave in NE Turkey (40°26'N; 39°32'E; 1530 m above sea level (asl)). The local climate, cave, and speleothem 2p are described by Jex et al. [2010, 2011]. Briefly, in this cave, spring snow melt initiates

Additional supporting information may be found in the online version of this article.

¹Water Research Centre, School of Civil and Environmental Engineering, University of New South Wales, Sydney, New South Wales, Australia.

²Connected Waters Initiative Research Centre, University of New South Wales, Manly Vale, New South Wales, Australia.

³Affiliated to the National Centre for Groundwater Research and Training (NCGRT) Australia.

⁴Climate Change Research Centre, University of New South Wales, Sydney, Australia.

⁵ARC Centre of Excellence for Climate System Science, University of New South Wales, Sydney, Australia.

⁶School of Geography, Earth and Environmental Sciences, University of Birmingham, Birmingham, UK.

Corresponding author: C. N. Jex, Water Research Centre, School of Civil and Environmental Engineering, University of New South Wales, Sydney, NSW 2052, Australia. (c.jex@unsw.edu.au)

©2013. American Geophysical Union. All Rights Reserved.
0094-8276/13/10.1002/grl.50467

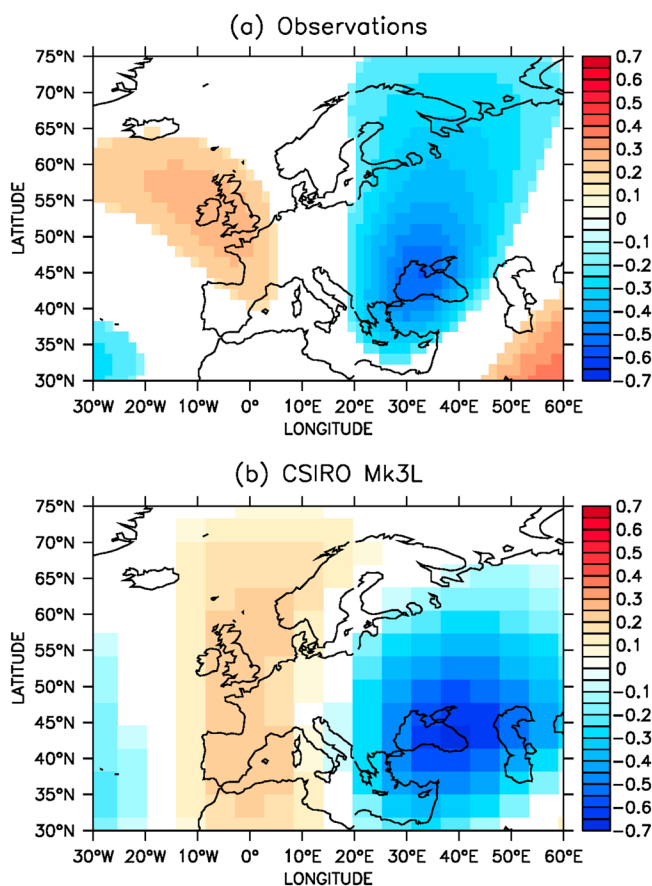


Figure 1. (a) Correlation between the amount of cool season precipitation recorded at Gümüşhane meteorological station (WMO station number: 17088, 40.45°N, 39.45°E, 1643 m asl) and 500 mb geopotential height using the ERA-40 reanalysis data between 1958 and 2004 A.D., resolution is $1.5^\circ \times 1.5^\circ$ ($p < 1\%$) [Uppala *et al.*, 2005]. Data were obtained from KNMI Climate Explorer (<http://climexp.knmi.nl>; accessed November 2012 [van Oldenborgh *et al.*, 2005]). (b) Correlation between simulated cool season precipitation at Gümüşhane and 500 mb geopotential height according to the CSIRO Mk3L model, diagnosed from a 10,000 year preindustrial control simulation.

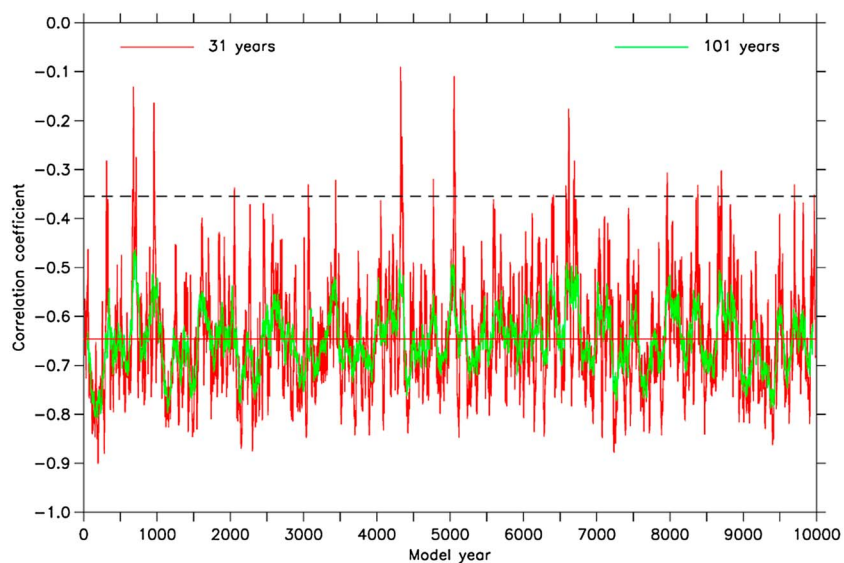


Figure 2. Running correlation coefficient between cool season precipitation at Gümüşhane and 500 mb geopotential height at 39°E, 43°N, diagnosed from a 10,000 year preindustrial control simulation conducted using the CSIRO Mk3L model: 31 years (solid red line) and 101 years (solid green line). The dark red horizontal line indicates the average value, and the broken line indicates the 95% significance level (± 0.354), for the 31 year running correlation.

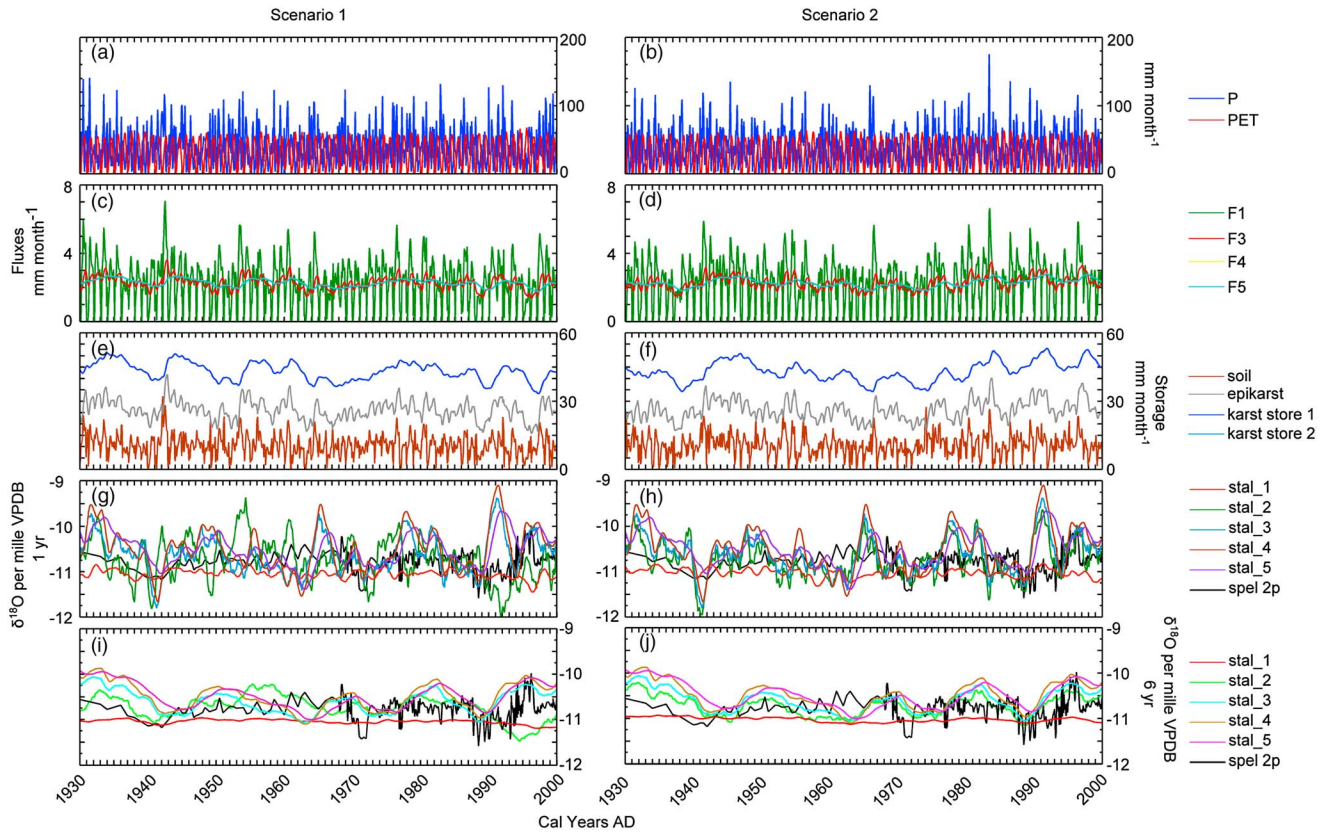


Figure 3. (a and b) Inputs, (c and d) fluxes, (e and f) storage, and (g–j) $\delta^{18}\text{O}_{\text{dw}}$ outputs using two contrasting model simulation input series (scenarios 1 and 2 of CSIRO Mk3L). The $\delta^{18}\text{O}_{\text{cmod}}$ outputs are smoothed by 1 year and 6 years to reflect the sampling resolution of the observed speleothem 2p (plotted as a thick black line in Figures 3g–3j).

infiltration into the karst aquifer, whilst in the warm season (May to September), infiltration is limited by a consistent seasonal soil moisture deficit [Jex *et al.*, 2010]. The relationship between the $\delta^{18}\text{O}_{\text{spel}}$ and the amount of cool season precipitation (i.e., falling in October, November, December, and January) throughout the instrumental period was established and subsequently the amount of cool season precipitation was reconstructed for the previous 500 years. A period of anomalously lower reconstructed rainfall at 1540–1560 A.D. was identified followed by a switch to lighter $\delta^{18}\text{O}_{\text{spel}}$ inferred as a period of increased rainfall in the late sixteenth century. The amount of cool season precipitation recorded at the local meteorological station was shown to correlate well with pressure fields in Western Russia (Figure 1a), which formed the basis of the paleoclimate interpretations.

[5] In this study, we address the two principal assumptions and sources of uncertainty in such paleoclimate reconstructions as follows:

[6] 1. That the dominant patterns of atmospheric circulation and the seasonal distribution of P have remained stable in nature throughout the period of study. We assess the stability of previously observed relationships between cool season precipitation and regional circulation dynamics at this speleothem site over the last 1 ka using the CSIRO Mk3L climate system model (section 2) [Phipps *et al.*, 2011, 2012].

[7] 2. That the statistical relationship between $\delta^{18}\text{O}_{\text{spel}}$ and the amount of cool season P have remained stable throughout the period of reconstruction. To avoid making this assumption, we use the T and P output of a three-member ensemble of transient climate model simulations and

synthetic $\delta^{18}\text{O}_{\text{pptn}}$ to drive the KarstFOR karst hydrology model. We investigate the variability in $\delta^{18}\text{O}_{\text{cmod}}$ that is explained by water storage and routing in the karst aquifer at this site over the last 1 ka (section 3) [Baker *et al.*, 2012].

2. Climatic Drivers of the Interannual Variability of Cool Season Precipitation

2.1. Correlations of Observed Climate to Large-Scale Atmospheric Circulation

[8] In the Near East, the influence of the North Atlantic Oscillation (NAO) on interannual precipitation and temperature trends is reported to be insignificant [Kutiel *et al.*, 2002; Türkeş and Erlat, 2003, 2005], and to our knowledge, no studies have found a significant correlation between precipitation in this region in any season and pressure centers that describe the NAO. Rather, the seasonal position of the Siberian high over Eastern Europe directly impacts upon temperature and precipitation patterns as well as dipole pressure centers over the North Sea and northern Caspian Sea. These demonstrate a robust correlation with the amount of cool season precipitation [Jex *et al.*, 2011] and temperature [Kutiel, 2011; Kutiel and Benaroch, 2002; Tatli, 2007] in the Near East region (Figure 1a).

2.2. Correlations of Simulated Climate to Large-Scale Atmospheric Circulation

[9] Details of the CSIRO Mk3L model and the simulations used in this study are provided in supplementary information. The model reproduces the observed climatology at

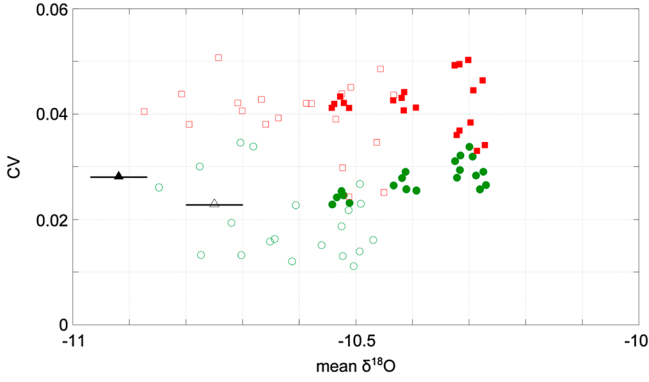


Figure 4. Mean versus CV of predicted $\delta^{18}\text{O}_{\text{cmod}}$ (red (1 year smooth) and green (6 year smooth) symbols) and $\delta^{18}\text{O}_{\text{spel}}$ (black triangles, with the solid bar indicating the associated analytical uncertainty). Solid symbols plot the statistics for the entire period of speleothem deposition (1500–1969 A.D.). Hollow symbols indicate statistics for the period 1970 to 2000 A.D. The data are split in this way, according to the speleothem sampling resolution. Speleothem 2p was sampled at a sub-annual resolution post 1969 A.D., but prior to this, the average sampling resolution is 6 years. Variability is captured well by the modeled $\delta^{18}\text{O}_{\text{cmod}}$ data smoothed by 6 years, regardless of whether the speleothem is sampled at a sub-annual resolution (1970 to 2000) or approximately 6 year resolution (1500–1969 A.D.). In particular, all model outputs for stal_2 drip site (fed by the epikarst store and 25% preferential flow component) plot most similarly to speleothem data over the instrumental. None of the predicted series plot close to the speleothem data when the earliest data are incorporated (1500–1969 A.D.), due to the discrepancy (up to 0.6‰) between the means.

the study site (Figure S1) and the relationship between cool season precipitation and the ONDJ 500 mb geopotential height (Figure 1b). This relationship is robust using both raw and smoothed data (Figure S2). Using raw data, a peak correlation of -0.65 occurs at 39°E , 43°N , one grid point to the north of the study site on the model grid. Figure 2 plots the strength of this relationship over the full duration of the 10,000 year control simulation. Generally the correlation is strong (up to -0.7) but there are periods of ~ 30 years when this correlation weakens substantially and becomes statistically insignificant at the 95% significance level, with correlation coefficients weaker than -0.35 . Thus, on periods longer than 30 years, the model suggests that the assumption of stationarity that underlies interpretations of $\delta^{18}\text{O}_{\text{spel}}$ at this study site is robust.

3. Non-Climatic Drivers of $\delta^{18}\text{O}_{\text{dw}}$ and $\delta^{18}\text{O}_{\text{spel}}$

3.1. KarstFOR Model Description and Setup

[10] We use the modified version of the *Bradley et al.* [2010] KarstFOR model, exactly as described by Baker et al. (manuscript in revision), to model stalagmite $\delta^{18}\text{O}$. A full description of the model, input and output data, and a model schematic is provided as auxiliary material. Briefly, the model envisages five water stores: (1) Soil, (2) Epikarst, (3) Karst Store 1, (4) Karst Store 2, and (5) an Overflow Store. Individual drip-water $\delta^{18}\text{O}$ series are produced by assuming that drip-waters are (1) solely derived from a particular water store (e.g., Stal_4), (2) the product of mixing of waters draining from a selection of water stores (e.g., Stal_1, _5, and _6), and (3) a combination of store drainage and recent precipitation $\delta^{18}\text{O}$ (arising through preferential flow through the soil and limestone) (e.g., Stal_2 and Stal_3). Stalagmite

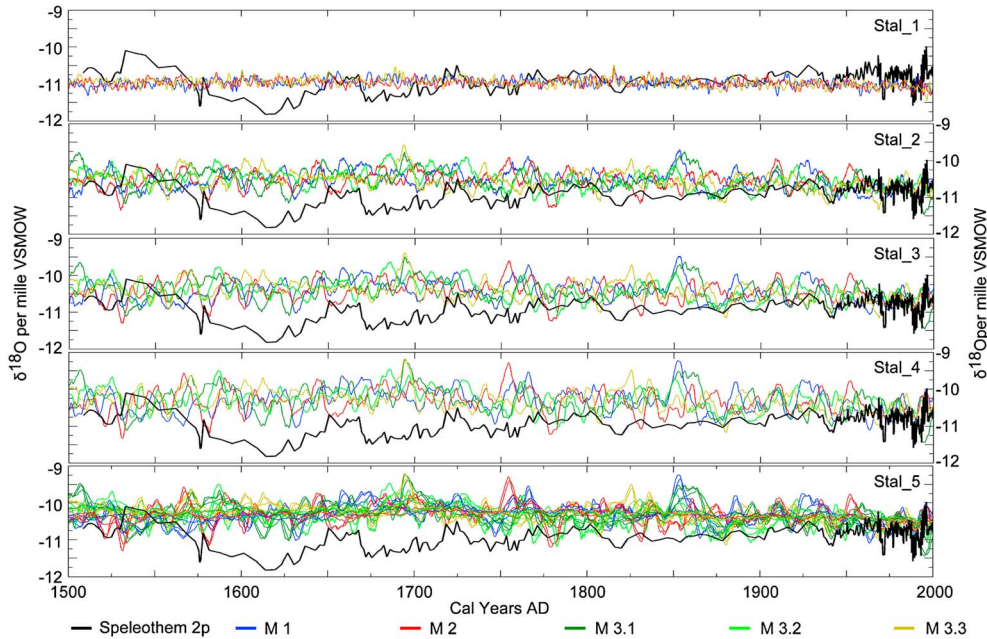


Figure 5. All predicted model runs $\delta^{18}\text{O}_{\text{dw}}$ for the full length of speleothem formation (1500–2000 A.D.). Each of the colored lines represents a different input series according to the three transient simulations of CSIRO Mk3L (M1 to M3.1). M3.2 and 3.3 use an alternative synthetic $\delta^{18}\text{O}_{\text{pttn}}$ to further test the variability of $\delta^{18}\text{O}_{\text{cmod}}$ associated with variable input series.

$\delta^{18}\text{O}$ series (Stal_1 to Stal_6 in Figure S3) are derived from each drip-water $\delta^{18}\text{O}$ series after allowing for calcite fractionation. As input data, we generated 1000 year synthetic climate series of monthly T, P, PET, and $\delta^{18}\text{O}_{\text{pptn}}$, representative of the local climate (see Text S2 in the auxiliary material). The karst model was set up with a -11.75% initial store value (obtained from stalagmite fluid inclusions at 6 ka) [Rowe *et al.*, 2012] and run for 1 ka, the last 500 years of which overlaps with the duration of growth of speleothem 2p.

3.2. Effect of Flow Routes and Storage Times in the Karst Aquifer

[11] A number of scenarios were completed for each input series, in which the storage capacity of each store was varied as well as their drainage functions (as summarized in Table S1). All KarstFOR output was smoothed by a 1 year running mean over the instrumental period (1938–2000 A.D.) and by a 6 year running mean for the entire record to reflect $\delta^{18}\text{O}_{\text{spel}}$ sampling resolution.

[12] We first present two contrasting examples of the model input series for the instrumental period from the GCM data, their fluxes (F1 to F7) and storage (soil, epikarst, and karst stores), and all of their predicted $\delta^{18}\text{O}_{\text{cmod}}$ series (Figure 3). Low P input and seasonally high evapotranspiration (ET) limit water stored in the soil ($<30\text{ mm month}^{-1}$ stored) and the subsequent water flux into the epikarst via F1 ($<8\text{ mm month}^{-1}$). The epikarst retains some seasonality in its total amount of storage, as does water flux F3, supplying karst store 1. The epikarst store maintains a supply of water to karst store 1 only, and to drip sites stal_2, _3, _4, and _5 throughout the period of speleothem deposition. In all but one of the scenarios, karst store 2 drains completely and yields no $\delta^{18}\text{O}_{\text{cmod}}$ output series at stal_1. Stal_6 remains dry throughout in all model runs and drainage scenarios (not shown). Varying the drainage functions and store sizes only impacts on $\delta^{18}\text{O}_{\text{cmod}}$ at stal_5 and stal_1 (the latter as summarized above). $\delta^{18}\text{O}_{\text{cmod}}$ at stal_5 is more variable with increasing drainage speed and is essentially a flat line under the slowest draining scenario (not shown). In all drainage and store size scenarios, predicted $\delta^{18}\text{O}_{\text{cmod}}$ for any one of the sites at stal_2, _3, and _4 is consistent. At these drip sites, only the initial input series and routing through the karst drives variability in their predicted $\delta^{18}\text{O}_{\text{cmod}}$ series.

3.3. Observed $\delta^{18}\text{O}_{\text{spel}}$ and Predicted $\delta^{18}\text{O}_{\text{cmod}}$ Over the Instrumental Period

[13] Figure 3 shows $\delta^{18}\text{O}_{\text{cmod}}$ plotted alongside the $\delta^{18}\text{O}_{\text{spel}}$ for the period 1930 to 2000 A.D. (data for all model runs are plotted in Figure S5). Once smoothed by a 6 year running mean, $\delta^{18}\text{O}_{\text{cmod}}$ for stal_2, _3, _4, and _5 in both of these model runs captures the low frequency (decadal scale) trends of the observed speleothem record during the twentieth century. However, in the 1 year smoothed data, only stal_2 and _3 (with a preferential flow component) capture the intra-annual variability as observed in the most recent portion of stalagmite 2p. Water from the epikarst store alone is too well mixed to predict observed speleothem variability on an intra-annual scale. Similarly, water from karst stores 1 (stal_5) and 2 (stal_1) (in the slowest draining scenario) is too well mixed to predict observed speleothem variability on an interannual scale.

[14] Plotting mean $\delta^{18}\text{O}$ against a measure of variability (coefficient of variation, CV) demonstrates that once smoothed by a 6 year running mean, predicted series for stal_2 in

particular have mean values and CVs most similar to the speleothem record for the instrumental period (Figure 4). This suggests that the intra-annual variability evident in the speleothem sampled at a sub-annual scale is likely to be a genuine reflection of routing through the karst aquifer in a manner most similar to that predicted at stal_2 and that integrated sampling effectively eliminates this intra-annual variability in the speleothem and the modeled drip water data of stal_2.

3.4. Observed $\delta^{18}\text{O}_{\text{spel}}$ Versus Predicted $\delta^{18}\text{O}_{\text{cmod}}$ Over the Last 500 Years

[15] The full range of $\delta^{18}\text{O}_{\text{cmod}}$ series from all model inputs is shown in Figure 5 for the entire 500 years of speleothem deposition (1500–2000 A.D.). The CV values of the model simulations for the entire record, smoothed by 6 years, agree well with that observed in the speleothem, sampled at this resolution. Mean values are, however, offset by as much as 0.5% (Figure 4). Whilst the model simulations predict reasonable $\delta^{18}\text{O}_{\text{spel}}$ values at the earliest and most recent parts of the speleothem record, no model run captures the transition from particularly heavy to light $\delta^{18}\text{O}_{\text{spel}}$ during the sixteenth and seventeenth centuries, based on any of the input series used. In such an evapotranspiration (ET) sensitive system, any changes to the amount or seasonality of ET would be expected to impact stal_2 and _3 with a preferential flow component. Based on the GCM data for P and T, no such change in ET is present. Possible explanations are

[16] 1. The speleothem is recording a localized climate signal that is not represented by the adjusted GCM input data or $\delta^{18}\text{O}_{\text{pptn}}$.

[17] 2. The GCM does not capture the true variability in cool season precipitation or temperature-related changes in ET at the study site, prior to the instrumental period.

[18] 3. A process not modeled in KarstFOR with these climate inputs is responsible for the shift in isotopic composition of this particular speleothem: for example, recharge by isotopically lighter groundwater during the late sixteenth and early seventeenth centuries that is not accounted for by the model input series (either the $\delta^{18}\text{O}_{\text{pptn}}$ or the estimated ET based on GCM data).

4. Discussion

[19] This paper tests the validity of a previously published speleothem-based climate reconstruction to provide a guide for how best to apply both climate system and proxy forward models to refine paleoclimate interpretations. The stability of observed relationships between the total amount of local cool season precipitation and regional circulation is assessed using the CSIRO Mk3L climate system model. Reductions in the amount of cool season precipitation and temperature are confirmed as resulting from increased pressure centered over the West Russia/Caspian Sea region, describing a scenario of negative NCP. This relationship is largely stable on millennial timescales, according to a 10,000 year preindustrial control simulation, giving credence to previous climatic interpretations of $\delta^{18}\text{O}_{\text{spel}}$. However, during this time, this relationship is observed to break down periodically on time scales less than 30 years.

[20] The output of multiple simulations of the CSIRO Mk3L climate system model for this location over the last 1 ka, combined with synthetic $\delta^{18}\text{O}_{\text{pptn}}$, was then used as input data for the KarstFOR hydrology model. We predict the range

of possible $\delta^{18}\text{O}_{\text{cmod}}$ that may occur given these inputs for a range of drainage scenarios and flow routes in the karst aquifer. The model generates $\delta^{18}\text{O}_{\text{cmod}}$ that matches $\delta^{18}\text{O}_{\text{spel}}$ over the instrumental period (1930–2000 A.D.). The range of observed interannual variability can be accounted for by the karst model given the GCM input data. However, the lightest values of $\delta^{18}\text{O}_{\text{spel}}$ during the late sixteenth and early seventeenth centuries and their subsequent transition to modern values cannot be accounted for by the GCM input to the karst model. This suggests that hydrological routing and storage of water cannot explain these particular trends. It is likely that isotopically lighter water recharged the aquifer at this time, which is not accounted for by the model input series of $\delta^{18}\text{O}_{\text{pptn}}$ or PET. If the former is true, then this does not necessarily mean that there was a substantial change to the amount of cool season precipitation, as originally inferred in the speleothem reconstruction of Jex *et al.* [2011]. One solution to the mismatch between proxy data and the karst model would be to use an isotope enabled regional climate model with the KarstFOR model embedded, as an alternative approach for generating a local $\delta^{18}\text{O}_{\text{pptn}}$ input series.

5. Conclusions

[21] We have identified and explored some of the sources of uncertainty that underlie the interpretation of speleothem $\delta^{18}\text{O}$ records. Using the published $\delta^{18}\text{O}_{\text{spel}}$ record from Turkey and the CSIRO Mk3L and KarstFOR models, we have been able to predict some key features of the observed speleothem record. This supports some of the original interpretations of the capability of this speleothem to reconstruct cool season precipitation and its relevance to understanding regional atmospheric circulation. Finally, we argue that for unambiguous interpretation of $\delta^{18}\text{O}_{\text{spel}}$ such an approach is necessary and that future methodological improvements include the use of process models such as KarstFOR, embedded within isotope-enabled general or regional circulation models.

[22] **Acknowledgments.** This work was funded by the University of New South Wales, Australia, and undertaken with the assistance of resources provided at the Australian National University through the National Computational Merit Allocation Scheme. The authors thank the reviewers for their thoughtful reviews of the manuscript.

[23] The Editor thanks Matthew Jones and an anonymous reviewer for their assistance in evaluating this paper.

References

- Baker, A., and C. Bradley (2010), Modern stalagmite $\delta^{18}\text{O}$: Instrumental calibration and forward modelling, *Glob. Planet. Change*, 71(3–4), 201–206.
- Baker, A., A. Asrat, I. J. Fairchild, M. J. Leng, P. M. Wynn, C. Bryant, D. Genty, and M. Umer (2007), Analysis of the climate signal contained within $\delta^{18}\text{O}$ and growth rate parameters in two Ethiopian stalagmites, *Geochim. Cosmochim. Acta*, 71(12), 2975–2988.
- Baker, A., C. Bradley, S. J. Phipps, M. Fischer, I. J. Fairchild, L. Fuller, C. Spötl, and C. Azcurra (2012), Millennial-length forward models and pseudoproxies of stalagmite $\delta^{18}\text{O}$: An example from NW Scotland, *Clim. Past*, 8, 1153–1167.
- Bradley, C., A. Baker, C. N. Jex, and M. J. Leng (2010), Hydrological uncertainties in the modelling of cave drip-water $\delta^{18}\text{O}$ and the implications for stalagmite palaeoclimate reconstructions, *Quaternary Sci. Rev.*, 29(17–18), 2201–2214.
- Cai, B., N. Pumijumong, M. Tan, C. Muangsong, X. Kong, X. Jiang, and S. Nan (2010), Effects of intraseasonal variation of summer monsoon rainfall on stable isotope and growth rate of a stalagmite from northwestern Thailand, *J. Geophys. Res.*, 115, D21104, doi:10.1029/2009JD013378.
- Jex, C. N., A. Baker, I. J. Fairchild, W. J. Eastwood, M. J. Leng, H. J. Sloane, L. Thomas, and E. Bekaroğlu (2010), Calibration of speleothem $\delta^{18}\text{O}$ with instrumental climate records from Turkey, *Glob. Planet. Change*, 71(3–4), 207–217.
- Jex, C. N., A. Baker, J. M. Eden, W. J. Eastwood, I. J. Fairchild, M. J. Leng, L. Thomas, and H. J. Sloane (2011), A 500 yr speleothem-derived reconstruction of late autumn–winter precipitation, northeast Turkey, *Quaternary Res.*, 75(3), 399–405.
- Kim, S.-T., and J. R. O’Neil (1997), Equilibrium and nonequilibrium oxygen isotope effects in synthetic carbonates, *Geochim. Cosmochim. Acta*, 61(16), 3461–3475.
- Kutiel, H. (2011), A review on the impact of the North Sea–Caspian Pattern (NCP) on temperature and precipitation regimes in the Middle East, in *Survival and Sustainability*, edited by H. Gökçekus, U. Türker, and J. W. LaMoreaux, pp. 1301–1312, Springer, Berlin, Heidelberg.
- Kutiel, H., and Y. Benaroch (2002), North Sea–Caspian Pattern (NCP)—An upper level atmospheric teleconnection affecting the Eastern Mediterranean: Identification and definition, *Theor. Appl. Climatol.*, 71(1), 17–28.
- Kutiel, H., P. Maheras, M. Türkeş, and S. Paz (2002), North Sea–Caspian Pattern (NCP)—An upper level atmospheric teleconnection affecting the eastern Mediterranean—Implications on the regional climate, *Theor. Appl. Climatol.*, 72(3), 173–192.
- Lohmann, G., A. Wackerbarth, P. M. Langebroek, M. Werner, J. Fohlmeister, D. Scholz, and A. Mangini (2013), Simulated European stalagmite record and its relation to a quasi-decadal climate mode, *Clim. Past*, 9(1), 89–98.
- Mattey, D., D. Lowry, J. Duffet, R. Fisher, E. Hodge, and S. Frisia (2008), A 53 year seasonally resolved oxygen and carbon isotope record from a modern Gibraltar speleothem: Reconstructed drip water and relationship to local precipitation, *Earth Planet. Sci. Lett.*, 269(1–2), 80–95.
- van Oldenborgh, G. J., M. A. Balmaseda, L. Ferranti, T. N. Stockdale, and D. L. T. Anderson (2005), Evaluation of atmospheric fields from the ECMWF seasonal forecasts over a 15-year period, *J. Climate*, 18(16), 3250–3269.
- Phipps, S. J., L. D. Rotstayn, H. B. Gordon, J. L. Roberts, A. C. Hirst, and W. F. Budd (2011), The CSIRO Mk3L climate system model version 1.0—Part 1: Description and evaluation, *Geosci. Model Dev.*, 4, 483–509.
- Phipps, S. J., L. D. Rotstayn, H. B. Gordon, J. L. Roberts, A. C. Hirst, and W. F. Budd (2012), The CSIRO Mk3L climate system model version 1.0—Part 2: Response to external forcings, *Geosci. Model Dev.*, 5, 649–682.
- Rowe, P. J., J. E. Mason, J. E. Andrews, A. D. Marca, L. Thomas, P. van Calsteren, C. N. Jex, H. B. Vonhof, and S. Al-Omari (2012), Speleothem isotopic evidence of winter rainfall variability in northeast Turkey between 77 and 6 ka, *Quaternary Sci. Rev.*, 45, 60–72.
- Sturm, C., Q. Zhang, and D. Noone (2010), An introduction to stable water isotopes in climate models: benefits of forward proxy modelling for paleoclimatology, *Clim. Past*, 6(1), 115–129.
- Tatli, H. (2007), Synchronization between the North Sea–Caspian pattern (NCP) and surface air temperatures in NCEP, *Int. J. Climatol.*, 27(9), 1171–1187.
- Türkeş, M., and E. Erlat (2003), Precipitation changes and variability in Turkey linked to the North Atlantic oscillation during the period 1930–2000, *Int. J. Climatol.*, 23(14), 1771–1796.
- Türkeş, M., and E. Erlat (2005), Climatological responses of winter precipitation in Turkey to variability of the North Atlantic Oscillation during the period 1930–2001, *Theor. Appl. Climatol.*, 81(1), 45–69.
- Uppala, S. M. et al. (2005), The ERA-40 re-analysis, *Quart. J. Roy. Meteor. Soc.*, 131(612), 2961–3012.
- Wackerbarth, A., D. Scholz, J. Fohlmeister, and A. Mangini (2010), Modelling the $\delta^{18}\text{O}$ value of cave drip water and speleothem calcite, *Earth Planet. Sci. Lett.*, 299(3–4), 387–397.
- Wackerbarth, A., P. M. Langebroek, M. Werner, G. Lohmann, S. Riechelmann, A. Borsato, and A. Mangini (2012), Simulated oxygen isotopes in cave drip water and speleothem calcite in European caves, *Clim. Past*, 8(6), 1781–1799.
- Yadava, M. G., R. Ramesh, and G. B. Pant (2004), Past monsoon rainfall variations in peninsular India recorded in a 331-year-old speleothem, *Holocene*, 14(4), 517–524.